The performances of expanded graphite on the phase change materials composites for thermal energy storage

Ibtissem Chriaa, Mustapha Karkri, Abdelwaheb Trigui, Ilyes Jedidi, Makki Abdelmouleh, Chokri Boudaya

The performances of expanded graphite on the phase change materials composites for thermal energy storage

Ibtissem CHRIAA[1]*, Mustapha KARKRI[2]**, Abdelwaheb TRIGUI[1], Ilyes JEDIDI[3], Makki ABDELMOULEH[3], Chokri BOUDAYA[1]

[1]Laboratoire des Matériaux Multifonctionnels et Applications (LMMA), Université de Sfax, Tunisie.

[2]Laboratoire CERTES, 61 avenue du Général de Gaulle, 94010 Créteil Cedex, Université Paris-Est, France.

[3]Laboratoire de Sciences des Matériaux et de l'Environnement (LMSE), Université de Sfax, Tunisie.

*Corresponding author: chriaa.ibtissem@gmail.com

**Co-corresponding author: mustapha.karkri@u-pec.fr

Abstract

For the storage of latent thermal energy (LTES), phase change materials (PCM) are the most commonly used. Nonetheless, their low thermal conductivity values and the liquid leakage on the transition phase of process limits their application. Hence, the stabilization-form can be a solution to surmount these two limitations. In this work, the Hexadecane with large latent heat was used as PCM, styrene-b-(ethylene-co-butylene)-b-styrene (SEBS) tri-block copolymer and the low-density polyethylene (LDPE) served as the supporting materials and expanded graphite (EG) was added for improving the thermal conductivity. We focused on the preparation of SEBS/ Hexadecane/ LDPE Composites and the improvement of the heat transfer using the EG. The Fourier Transformation Infrared spectroscope also demonstrated a good compatibility between SEBS, LDPE, Hexadecane, and EG. The transient Guarded Hot Plate Technique (TGHPT) and a Thermogravimetric analyzer were utilized to assess the thermal properties and thermal stability of the PCM composites respectively. Further, a leakage test proved that the composite has an excellent form-stable property. Thanks to expanded graphite, no hexadecane leakage was depicted at a 75% mass fraction of PCM in composites, which surmounts almost all mass fraction values reported in the literature.

Keywords

Composite PCM, Thermal energy storage, Expanded graphite, Heat transfer, styrene-b-(ethylene-co-butylene)-b-styrene.

1. Introduction

Recently, the phase change materials (PCMs) have been widely used thanks to their high thermal energy storage (TES) capacity. Several works have proved its ability to reduce the energy consumption [1, 2]. Among the multifarious methods for thermal energy storage [3], the latent thermal energy storage (LTES) is notably efficient because of the small temperature differential between stored and released heats and its higher storage density [4]. PCMs belong to LTES materials which can absorb or release heat over the phase transition process, thanks to their great storage density and low temperature variation from storage to retrieval [5,6]. They are divided into organic and inorganic classes [7]. Notably, the organic PCM type, such as paraffin, has the advantages over inorganic PCMs due to important latent heat, small vapor pressure and great chemical stability [8]. The Hexadecane ($C_{16} H_{34}$) is a type of alkanes (PCM). Compared with other thermal energy storage materials, the use of hexadecane has numerous benefits such as its phase transition temperature (18 °C) close to room temperature and its important latent heat (224 J/g) [9]. Nevertheless, the low heat transfer values and the liquid leakage on the phase change process limits its use in thermal energy storage (TES) applications. To surmount these problems, several strategies have been investigated [5]. First, the adsorption of PCM by porous materials of shape-stabilized composites, such as porous carbon materials has been used [10]. As well, the expanded graphite is the most employed thanks to its great thermal absorbability and its high

thermal conductivity [11]. Second, microencapsulation of the PCM *in situ* or interfacial polymerization is another efficient approach [12]. This technique presents some problems such as the melted PCM leakage once a core and the capsule shell of encapsulated PCM crack [5]. Lastly, PCM is directly embalmed into polymer supports to develop form-stable composites [13]. Many polymers following the strategy of form stable PCM, such as polyacrylate [14, 15], polyurethane [16], and polyolefin [17, 18], can be used as supporting materials. The low thermal conductivity of PCM based on polymer materials is another drawback because the high thermal conductivity can accelerate the storage and release of thermal energy. To improve thermal conductivity, Krupa et al. [19] prepared a composite based on a PCM, LLDPE and graphite using the uniaxial cold compression method. They reported a remarkable improvement in the composite's thermal conductivity compared to the pure PCM. Sobolciak et al. [20] investigated the thermal and mechanical properties of PCM based on LLDPE, paraffin wax and EG. They concluded that the incorporation of EG particles into the blends improved the mechanical properties. Merlin et al. [21] indicated that these conventional polymers based on form stable PCM exhibit high shape stability, it still faces the installation difficulty problem generated by the strong rigidity and no flexibility of the material.

Many explorations on thermoplastic elastomer supporting materials (e.g. SEBS, SBS, OBC …) are available. Chriaa et al. [22] investigated the effect of the elastomer SEBS in the thermal properties of Hexadecane/LDPE composites. They concluded that the elastomer (SEBS) exhibited good absorption and encapsulation to Hexadecane and that the mass fraction of Hexadecane could reach approximately 80% with a good form stability, which surmounts almost all mass fraction values reported in the literature. Wu et al. [23] prepared a form stable PCM based on the PA, OBC, and EG. OBC was used as the supporting material to avoid the leakage of liquid PA and the porous GE with porous characteristic to improve the thermal conductivity. They concluded that prepared form stable PCM has capacities of thermal induced flexibility and enhanced thermal conductivity, which ensure promising applications in the TES and TM.

In this work, a new composite PCM based on Hexadecane, LDPE, SEBS and EG was prepared by sonication method. LDPE served as a solid supporting material, whereas SEBS showed a good encapsulation of hexadecane. The expanded graphite was employed to create the thermal conductive networks inside the shape stabilized PCM composite. Samples with several

masses of LDPE and EG were assessed in terms of thermal conductivity, thermal stability, and chemical composition. Based on the obtained results, the composites open very wide horizons in the thermal energy storage and thermal management applications.

2. Materials and methods

2.1 Materials

Hexadecane ($C_{16}H_{34}$, Sigma Aldrich with 99% purity), a saturated hydrocarbon of the alkane's family with a phase change temperature of 18-20°C, was used as the PCM thanks to its high latent heat (over 224 kJ/kg). Elastomer SEBS (Kraton G1650 M, linear tri-block copolymer based on styrene and ethylene/butylene with a polystyrene content of 30%) and the LDPE were selected as the supporting materials for their good compatibility with Hexadecane. Expanded graphite (EG) was supplied by Sigma Aldrich. Toluene (C_7H_8, analytical reagent, Sigma Aldrich) served as solvent.

2.2 Preparation

A series of the SEBS/Hexadecane/LDPE composites modified by EG was prepared using a sonication process (**Fig. 1**). Firstly, the Hexadecane (PCM) was melted by heating at 80°C. The SEBS and the LDPE were mixed in the liquid PCM. This solution was added to 60 ml of toluene and stirred at a speed of about 800 rpm at 80 °C to yield a homogeneous solution. The EG was added to the solution (at 80°C for 30 min). Sonication was then applied (20 min at 120 W) to decompose the graphite aggregates and obtain a homogeneous dispersion of the micro-particles. Then, the mixture was left under a hood at 120°C to evaporate the toluene. Next, the composite PCM was dried at 130°C inside a vacuum oven overnight to eliminate the liquid Hexadecane which did not adhere to matrix polymer. Finally, the solution was injected in a mold of 45 mm in diameter for hot-pressing. This technique produced parallelepiped-shaped composites with different mass fractions of EG, as shown in **table 1**.
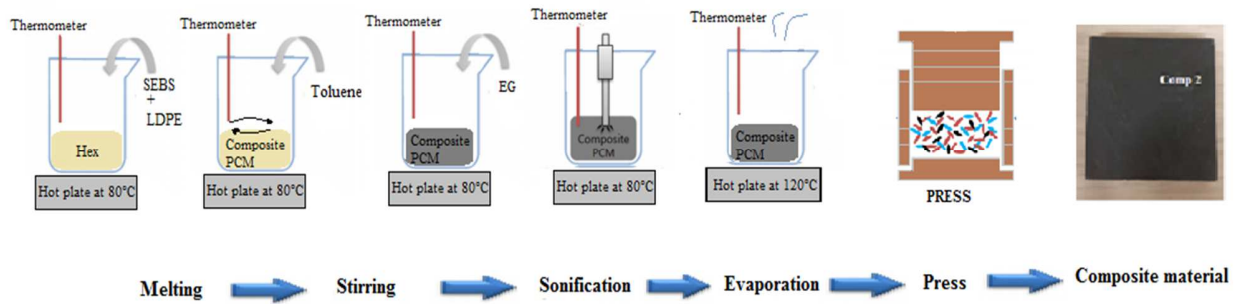
Fig. 1. The process of preparing the composite material

Table 1: The composition of the SEBS/ Hexadecane/ LDPE/ EG composites.

	SEBS (Wt. %)	Hexadecane (Wt. %)	LDPE (Wt. %)	EG (Wt. %)	Thickness (mm)	Mass (g)
S0	15	75	10	0	5.70	8.904
S1	15	55	30	0	6.02	9.154
S2	15	45	40	0	6.05	9.257
S3	15	75	5	5	6.01	8.669
S4	10	75	5	10	5.94	9.006
S5	5	75	5	15	6.08	9.593
S6	15	45	35	5	5.82	8.928
S7	15	45	30	10	6.08	9.392
S8	15	45	20	20	6.12	9.628

2.3 Characterization

2.3.1 Chemical characterization

Fourier transform infrared spectroscopy (FT-IR) was used to analyze the chemical structure of the PCM composite at a spectral range of 400-4000 cm^{-1}.

2.3.2 Thermal properties

To evaluate the shape stability, the composite efficiency and life span, the leakage test was used. The experiment was realized by placing the composite with initial mass M_0 on a layer of filter paper in an oven at 50°C. After one hour, the sample was taken out and weighted using an analytical balance after cooling down to room temperature with the filter paper replaced following each weighing. M_n presents the mass of the sample after heating in the oven for n times and the leakage rate could be calculated as:

$$L\ (\%) = \frac{(M_0 - M_n)}{M_0} * 100 \tag{1}$$

The thermal conductivity of the composites with different loadings was measured by the Hot Disk Thermal Constant Analyzer (TPS 2500S) using a transient plane source method with a precision of ± 5%. A spiral-type heating source was located at the center of the sensor between two identical samples [23, 24]. The thermal conductivity test was performed under room temperature (24°C, under which hexadecane is at liquid state) and at 14°C (under which hexadecane is at solid state).

The thermal stability of composites PCM was tested by a thermo-gravimetric analyzer (TGA, PerkinElmer) under a constant stream of nitrogen with a linear increment of 20°C/min under nitrogen atmosphere.

By the Transient Guarded Hot Plate Technique (TGHPT), the composites thermal properties were determined (Fig.2). A parallelepiped-shaped sample (4,5 x 4,5 x 0.6 cm³) was located between two isothermal aluminum heat exchanger plates connected to thermo-regulated baths that allowed the fine regulation of the temperature of the injected oil H10 with a precision of approximately 0.1°C. Heat flux sensors and thermocouples (type T) were placed on each side of the composite sample to measure the heat flux $\Phi_{1,2}$ and temperature $T_{1,2}$ on each face of the LDPE/Hexadecane/SEBS composite. The lateral sides of the samples were insulated with polyethylene-expanded foam (PE) **[25, 30]**. The sensors were connected to LabVIEW software to measure temperature fluctuations and heat flux exchanged during melting and solidification processes. Experimental data were recorded at regular and adjustable time steps (1*s*-6*s*).
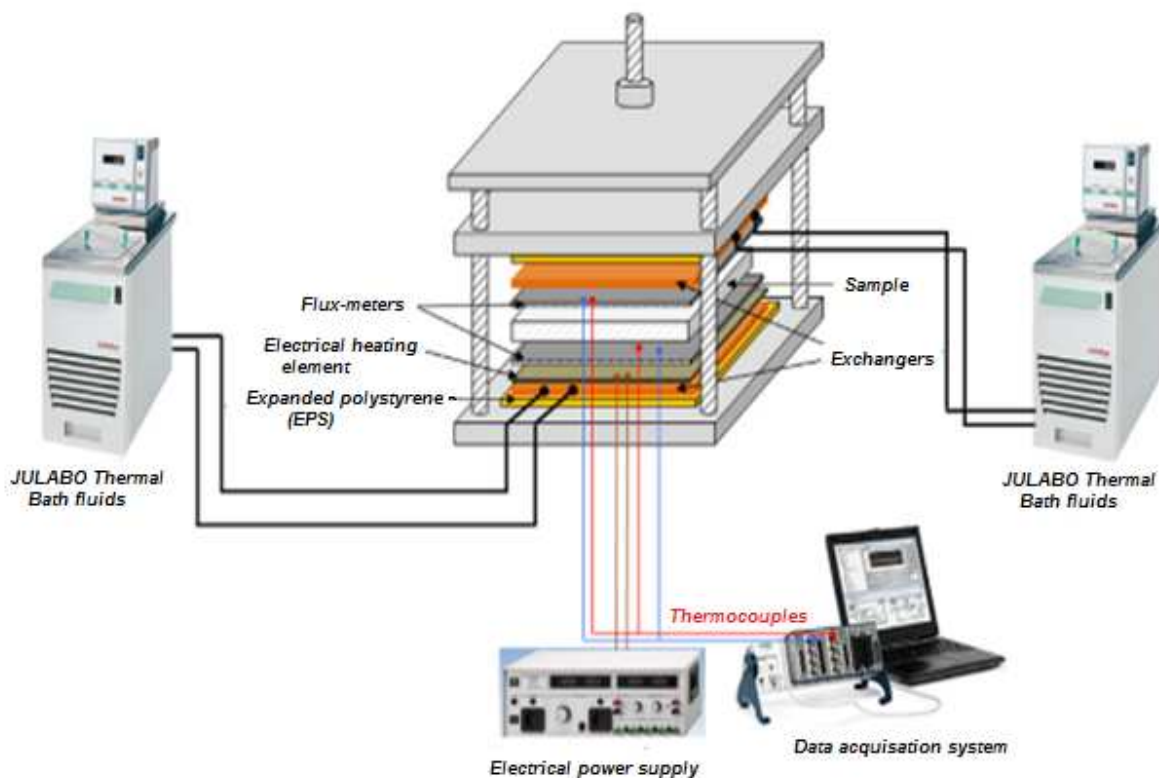
Fig. 2. Transient Guarded Hot Plate Technique (TGHPT).

3. Results and discussion

3.1 Chemical composition

The FT-IR spectra from 400 to 4000 cm^{-1} of SEBS, LDPE, S0, S3 and S5 are exhibited in **Fig. 3**. The spectrum of the LDPE shows four main peaks at 2933 cm^{-1}, 2864 cm^{-1}, 1457 cm^{-1} and 717cm^{-1}, which are assigned to $-CH_2$ symmetric stretching, $-CH_3$ symmetric stretching, $-CH_2$ deformation vibration and $-CH_2$ rocking vibration respectively. Nevertheless, the SEBS infrared absorption peaks were very small compared to those of LDPE. As depicted in the spectrum of S0, the peaks at around 2931 cm^{-1} and 2862 cm^{-1} are ascribed to the $-CH_2$ asymmetrical stretching vibration and symmetrical stretching vibration respectively. The peaks at 1463 cm^{-1} and 724 cm^{-1} are assigned to the $-CH_2$ rocking vibration and the peak at 1356 cm^{-1} resulted from the deformation vibration of $-CH_3$. It could be seen that peaks in S0 spectrum evidently show both the characteristic peaks of n-hexadecane [31] and LDPE. Furthermore, the spectra of S3 and S5 are like those of S0. No modifications appeared in the principal absorption peaks of

LDPE/Hexadecane/SEBS/EG composites. We concluded that there was no chemical reaction between the SEBS, hexadecane, LDPE and EG.
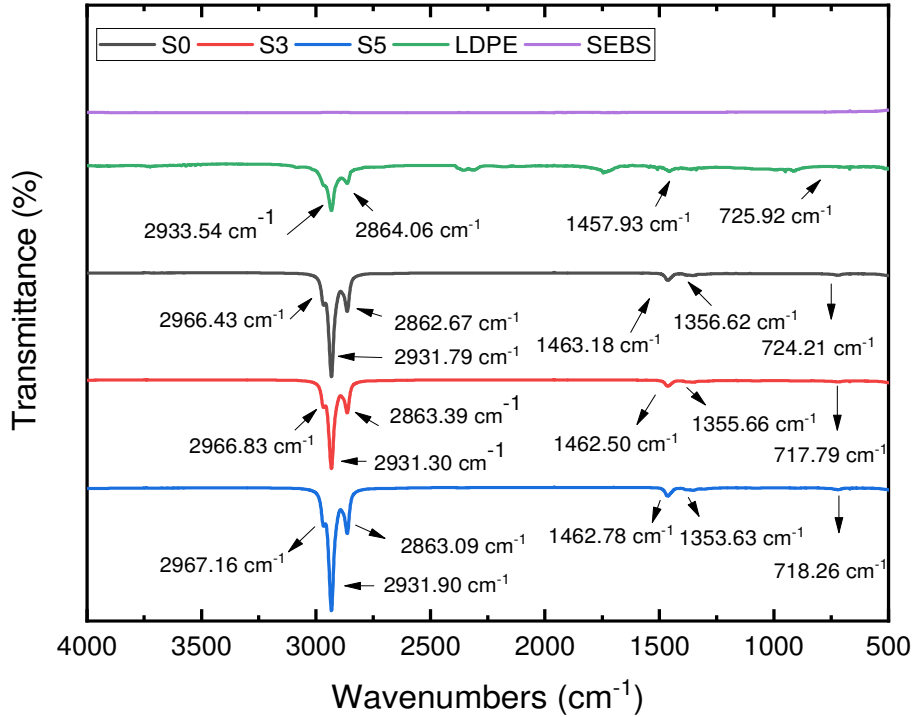

Fig. 3. FT-IR Spectrum of LDPE, SEBS, S0, S3 and S5 composites.

3.2 The shape stability of composite

The shape stability of the three composites series with and without EG was investigated by a leakage test as described in section 2.3.2. **Fig. 4** shows the weight loss of S0-S8 over the number of cycles. As seen from **Fig. 4. a**, the hexadecane leakage rate of S0 gradually increases with the cycle number and there are some imprints appear around this sample after thermal treatment. Some imprints appeared around this sample after thermal treatment **(Fig. 5)**. The variations of L (%) as a function of time were plotted, which can be expressed by a fitting linear equation:

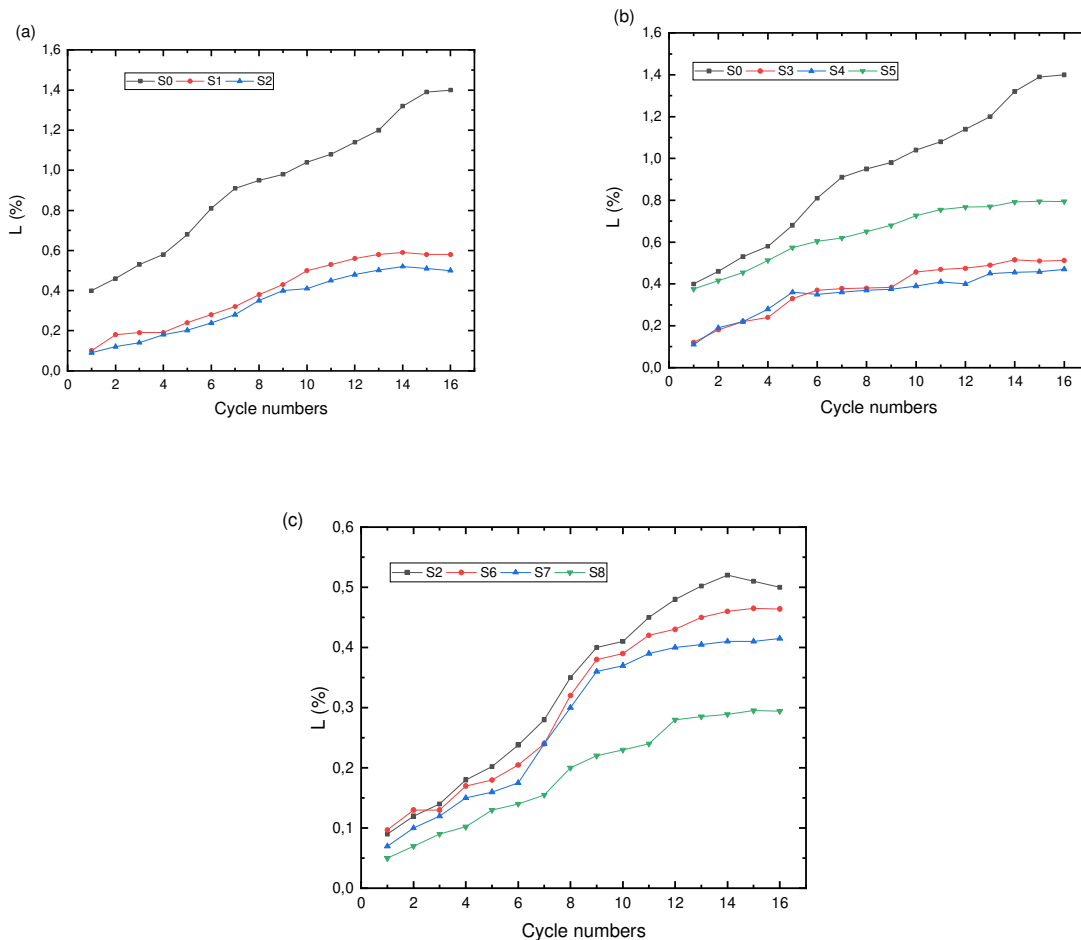$$L\ (\%) = 0.\ 35 + 0.068.t\ (R^2 = 0.9934) \tag{2}$$

Fig. 4. Leakage test of S0-S8 samples over heating cycle numbers.

The equation above indicates that at least 100 cycles are requisite to lose 6 wt. % of hexadecanes. S1 and S2 blends showed comparable performances with a very low leakage ratio. Both composites did not show any leakage starting from the tenth cycle when the polymer ratio was equal to or lower than the PCM ratio **[11]**.

In addition, according to **fig. 4.b**, the leakage was below 0.6 % after 10 heating cycles. It can be concluded that the EG improved the shape stability of S0 composite with an important amount of hexadecane. This amelioration can be attributed to the capillary and surface tension actions of its network-like porous structure **[32]**. The photographs **in fig.5** show some imprints around S0 and low imprints around S4 after thermal treatment. However, the leakage test proves that S4 has a good shape stability compared to S5. the composite with 15 wt. % EG recorded a leakage ratio higher than S3 and S4. This result can be explained by the low percentage of polymer matrix

(SEBS/LDPE). In the S2 composite, the leakage ratio was very weak compared to S0. The EG does not have an important effect on the stability form of this type of composite (Fig.4. c). This can be explained by the important amount of LDPE allowing to encapsulate the Hexadecane content.

Before heating

After heating

(50°C)
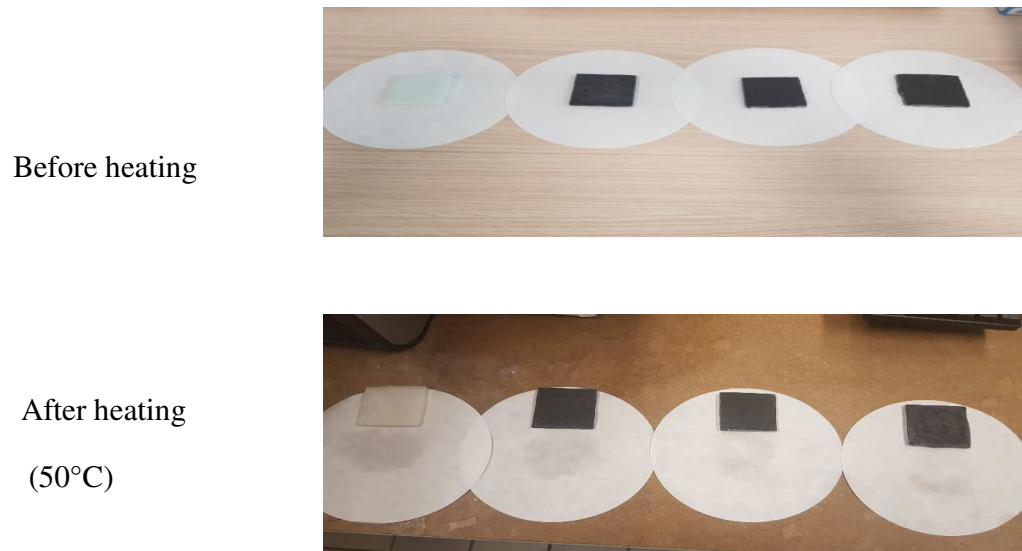
Fig. 5. Shape-stable photographs of the S0, S3, S4, and S5 before and after heating cycles.

3.3 Thermal conductivity and diffusivity results

Table 2 summarizes the measured thermal conductivities, diffusivities and associated uncertainties of the composites with different hexadecane contents. The heat transfer was reduced with increasing hexadecane loading. For example, thermal conductivity declined from 0.2441 W/m. K (45 wt. % hexadecane) to 0.1843 W/m. K (75wt. % hexadecane) at T= 23°C (room temperature). This phenomenon is explained by hexadecane thermal properties and molecular structure, which give it the role of an insulator compared to the polymer matrix LDPE/SEBS.

Table 2: The thermal conductivities and thermal diffusivities of PCM composites

Samples	Hex. (Wt. %)	EG (Wt. %)	$\acute{K}_{eff}$ (W/m. °C)	$\Delta\acute{K}_{eff}$ (W/m. °C)	α_{eff} (mm^2/s)	$\Delta\alpha_{eff}$ (mm^2/s)	$I_{\acute{K}eff}$ (%)
S0	75	-	0.1843	0.0092	0.1194	0.0059	-33
S1	55	-	0.2242	0.0112	0.1412	0.0070	-18
S2	45	-	0.2441	0.0122	0.1511	0.0075	-11
S3	75	5	0.3789	0.0189	0.1422	0.0071	38
S4	75	10	0.7478	0.0373	0.2102	0.0102	172
S5	75	15	1.0367	0.0518	0.3112	0.0155	277
S6	45	5	0.4825	0.0240	0.2082	0.0104	75
S7	45	10	0.9451	0.0472	0.2520	0.0126	244
S8	45	20	1.2402	0.0670	0.3829	0.1914	351

To improve the heat transfer in LDPE/Hexadecane/SEBS composites, the EG was added to composite S0 (75 wt. % hexadecane) and S2 (45 wt. % hexadecane). **Fig 6.a** shows the thermal conductivity of LDPE/ 75 wt. % hex/SEBS samples. The wt. % EG augmented from 0 to 15 wt. %. The measured thermal conductivity of the sample S5 (with 15 wt. % EG) increased to 1.0367W/m.K while the sample without graphite thermal conductivity was only 0.1843 W/m. K. It is noteworthy here that the thermal conductivity increased almost linearly with EG mass fraction. By a fitting linear equation, this variation can be expressed as follows:

$$Y = 0.17621 + 0.05208.x \qquad (3)$$

Where y is the composite thermal conductivity, x is the EG mass fraction and the correlation coefficient of eq. (3) is 0.98568. The EG improved the thermal properties of the composite LDPE/Hexadecane/SEBS composites thanks to the higher values of pure EG thermal conductivity. for composites with 45 wt. % hexadecane, a similar result was obtained (**Fig. 6.b**).

The thermal conductivity intensification obtained by the addition of graphite was calculated by eq. (4).

$$I_{\Lambda\,eff} = (\Lambda_{eff} - \Lambda_m)/\Lambda_m \qquad (4)$$

Where Λ_{eff} is the effective thermal conductivity of composite and Λ_m is the thermal conductivity of the matrix (LDPE/SEBS). The composite intensification of composite S3 with 75 wt. % hexadecane increased from 38 % to 277 % with increasing EG loading (5 to 15 wt. %). A similar comportment was obtained for composite containing 45 wt. % hexadecane with an intensification of 351 % (20 wt. % EG).
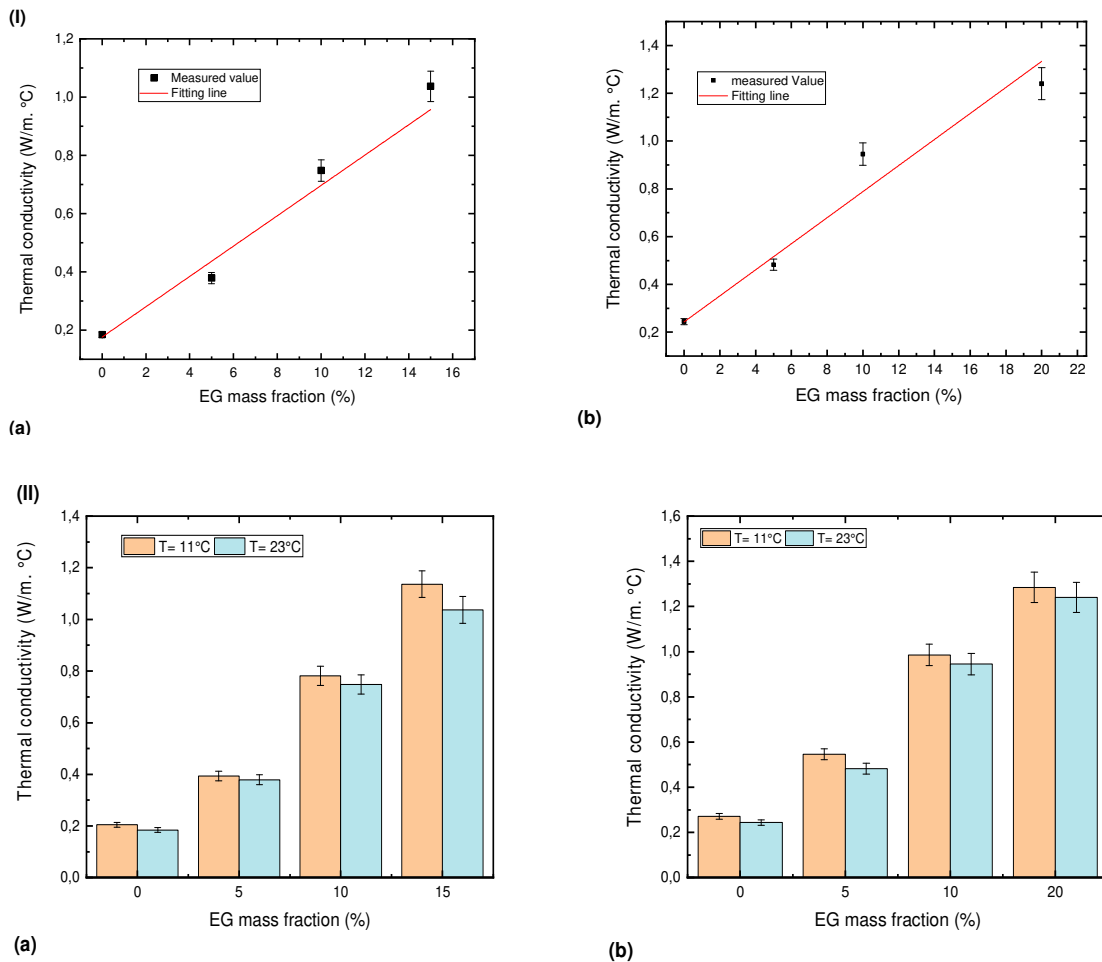

Fig. 6. Thermal conductivities as a function of: (I) various loadings of expanded graphite and (II) with different temperatures of composites containing 75 wt. % PCM (a) and composites containing 45wt. % PCM (b).

The thermal properties of the LDPE/ Hexadecane/SEBS composites without and with EG in both liquid and solid states were measured at 23°C and 11°C respectively **(Fig. 6 (II)).** At the same Hexadecane mass fraction, the thermal conductivity in the solid state outweighed the liquid state. Obviously, this phenomenon can be explained by the crystalline destruction of hexadecane during the transition from solid to liquid states **[33]**. Thus, in our study, the prepared composite modified by the graphite had a recommendable thermal conductivity which is desirable for application in TES systems.

3.4 Thermogravimetric analysis

The thermogravimetric analysis was performed to evaluate the degradation of the as-prepared composite. The test temperatures ranged from 25°C to 600°C (heating rate 20°C/min). As seen from **fig. 7.a** and **fig. 7.b**, the weight curve of LDPE and SEBS present a mainly degraded in one step. The degradation of these polymers began at around 350°C and finished at around 500°C. The thermal degradation of composites was a two-step process, which is typical for immiscible mixtures of different degradation temperatures. The first step ranged from 250°C to 320°C, corresponding to the degradation of hexadecane. The mass loss percentage for this stage corresponds to the hexadecane quantity mixed in the composite S0. The second step at above 400°C signifies the degradation of LDPE/SEBS polymer matrix. However, the hexadecane mass ratio in S1 and S2 composites was less than the PCM amount incorporated into the polymer support (LDPE/SEBS) during the preparation of the composite. This result confirms that LDPE/SEBS matrix can only preserve a fraction of the hexadecane if the PCM is incorporated with a higher weight percentage of the matrix **[34]**.

After adding EG (**Fig 7.c and Fig 7.d**), a similar phenomenon was observed, while a char layer was formed above 500°C. During the analysis of the residue at 600°C, the EG amount was found to be the same as the initial value. Consequently, the EG improved the thermal stability of composites owing to the chain mobility reduction and degradation inhibition [11].

3.5 The heat capacity in liquid and solid states

To determine the sensible heat and specific heat capacity of composites, the method used here consists of simultaneously measuring the temperatures T_1, T_2 and the heat fluxes φ_1 and φ_2 of

the two surfaces of the composite (T_1 and T_2 are two thermocouples integrated in the flux meters).
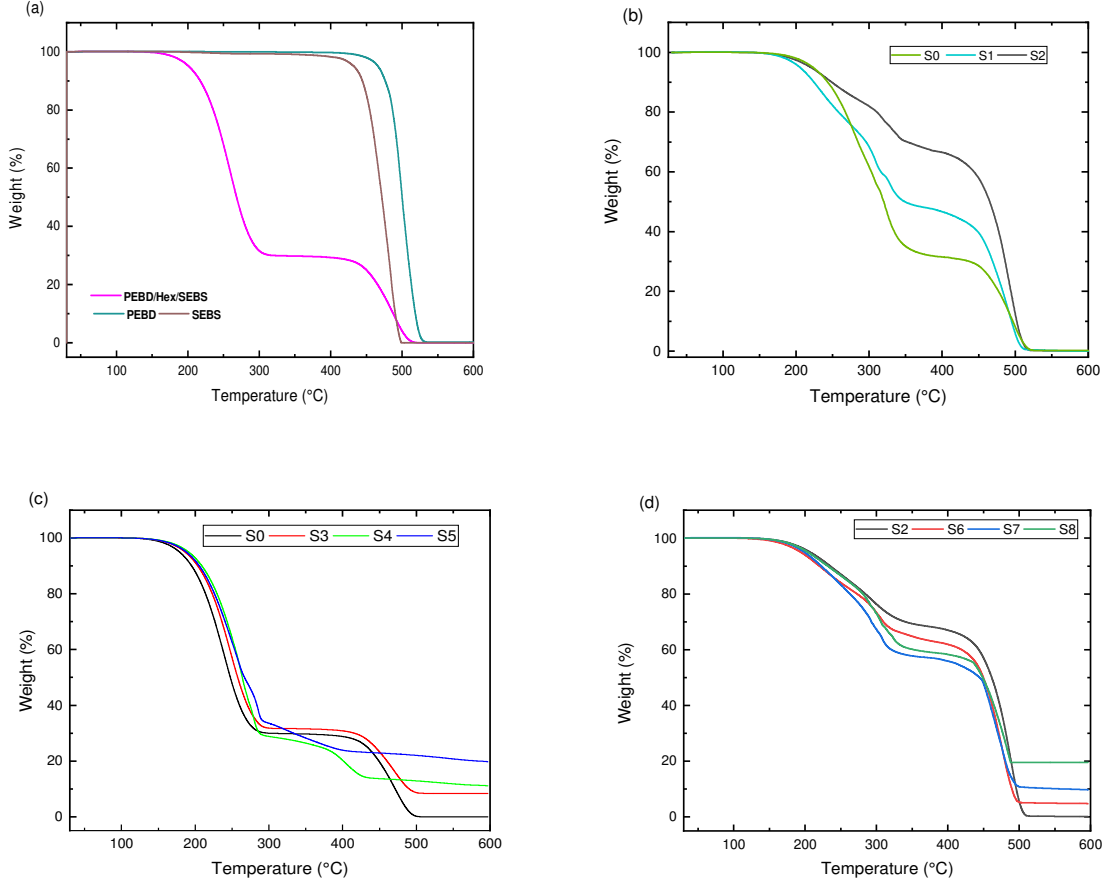

Fig. 7. TGA curves of (a) SEBS, LDPE, S0, (b) S0-S2, (c) S3-S5 and (d) S6-S8.

At the beginning, the two heat exchange plates and the composite were maintained at a constant temperature T_{init} (isothermal state). By means of the exchange plates, the composite evolved to a steady isothermal final temperature T_{end}. Between these two isothermal states, the PCM composite stored an amount of heat Q_{sens} which represents the internal variation of the system's energy **[30, 35]**. The assessment of the specific heat capacity is conducted by calculating the integral of the heat flux difference from the initial state (t_{init}) and the final state (t_{end}).

$$Q_{sens} = \frac{1}{\rho.e} \int_{t_{init}}^{t_{end}} \Delta\varphi.dt = C_p.(T_{end} - T_{init}) \tag{5}$$

Where C_p is the specific heat, $\Delta\varphi$ is the difference heat flux measured at each time step during the acquisition dt, e is the composite's width and ρ is its density.

To evaluate the 'storage' process, Different tests were carried out:

1. The temperature was checked from T_{init} = 20 °C to T_{end} = 33 °C to determine the sensible and specific heats of the compound in the liquid state.
2. The temperature was varied from T_{init} = 5 °C to T_{end} = 11 °C to determine the sensible and specific heats of the compound in the solid state.
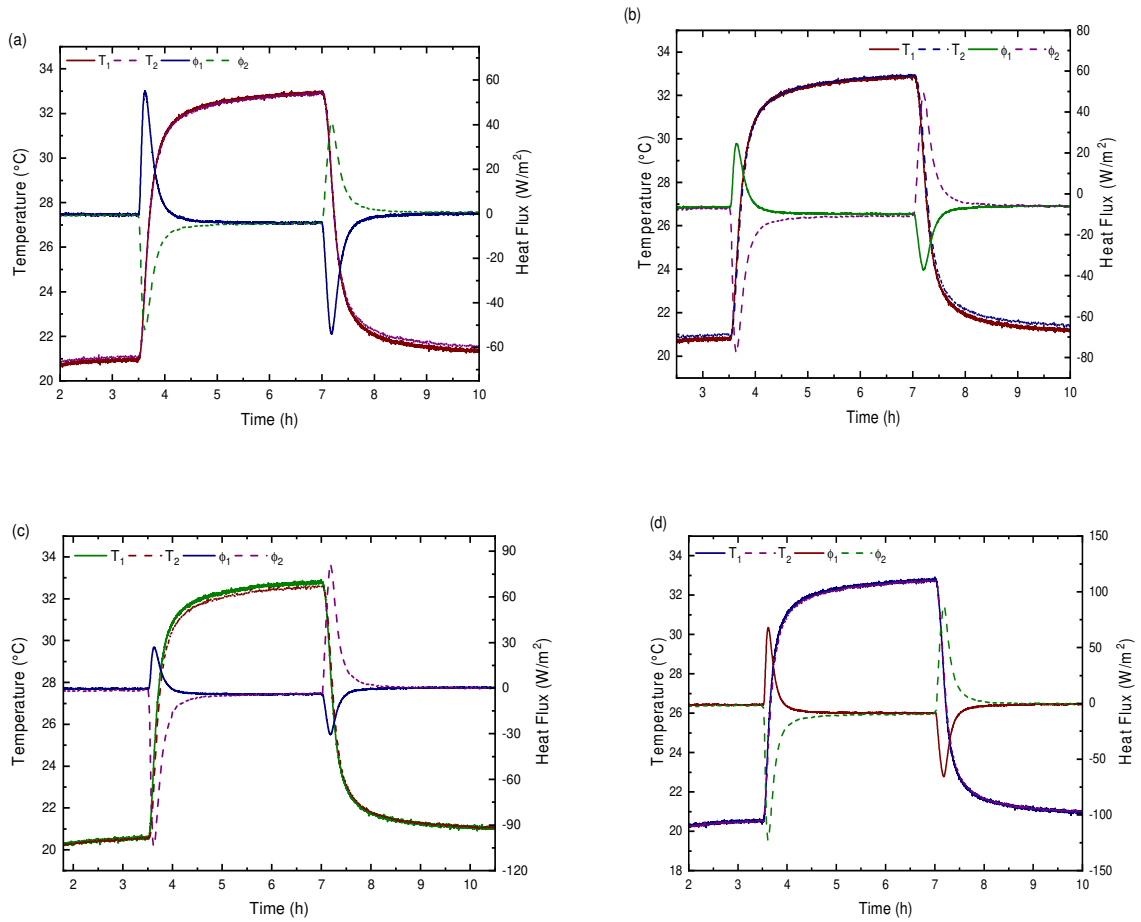

Fig. 8. Heat flux and temperature evolution of composites at liquid state (a) S0, (b) S4, (c) S2 and (d) S7.

Fig. 8 illustrates the heat flux progress as a function of temperature corresponding to the liquid state of S0, S4, S2 and S7. Initially, S0 was maintained at a constant initial temperature T_{init} = 20°C. Next, the temperature increased to T_{end} = 33 °C. For the sample to reach a thermal equilibrium state, a stabilizing time was requisite after every temperature-imposed change. Then, the composite was cooled down to T_{init} = 20 °C. The same experimental procedure was applied by choosing T_{init}= 5°C and T_{end} = 11°C To investigate the specific heat in the solid state of composite.

According to **table 3**, the addition of Hexadecane in the LDPE/SEBS matrix was proved to improve the specific heat capacity in both states. The specific heat increases with decreasing hexadecane mass ratio in the composites. Thus, the composite specific heat capacity in the solid state was not like that in the liquid state. A Slight decrease in C_p results is expected with increasing EG loading. Sobolciak et al. **[33]** showed that the specific heat decreased with increasing EG content. This result can be explicated by the lower graphite specific capacity, which was approximately 0.75 kJ/ kg. °C.

Table 3: Thermal heat capacity C_p and sensible heat Q_{sens} of the investigated composites.

Samples	Q_{sens} (kJ/kg)		C_p (kJ/ kg. °C)	
	Solid	Liquid	Solid	Liquid
S0	9,9731	19.951	2.6245	2.1002
S1	12.239	20.853	3.2209	2.1950
S2	13.974	23.168	3.6775	2.4388
S3	9.9962	20.073	2.6306	2.1130
S4	9.4977	19.081	2.4994	2.0086
S5	9.4441	19.068	2.4853	2.0072
S6	13.201	22.822	3.4741	2.4024
S7	13.002	22.732	3.4217	2.3929
S8	12.569	21.956	3.3078	2.3113

3.6 Energy storage and release

For thermal energy storage applications, the amount of total energy storage/release can be calculated by a temperature variation from 10°C to 33°C. **Fig. 9** shows three heating/cooling cycles of 3 h. 30 min to allow the composite to reach its state of thermal equilibrium. First, the composite S4 was maintained at initial temperature T_{init} = 10 °C, inferior to the phase change point of Hexadecane. Then, it was heated to T_{end} = 33 °C ((a), (c), (e)). The composite stored a latent and sensible heat among these two isothermal states. It is notable here that a stabilization time is necessary for temperature regulation. To finish, the sample was cooled to the T_{init} = 10 °C ((b), (d), (f)). The thermal evolution from 10 °C to 33 °C allowed monitoring the complete melting process during which a great amount of heat was stored by the material. From these results, the total heat can be calculated six times (Three times during the storage process and three times during the release process).
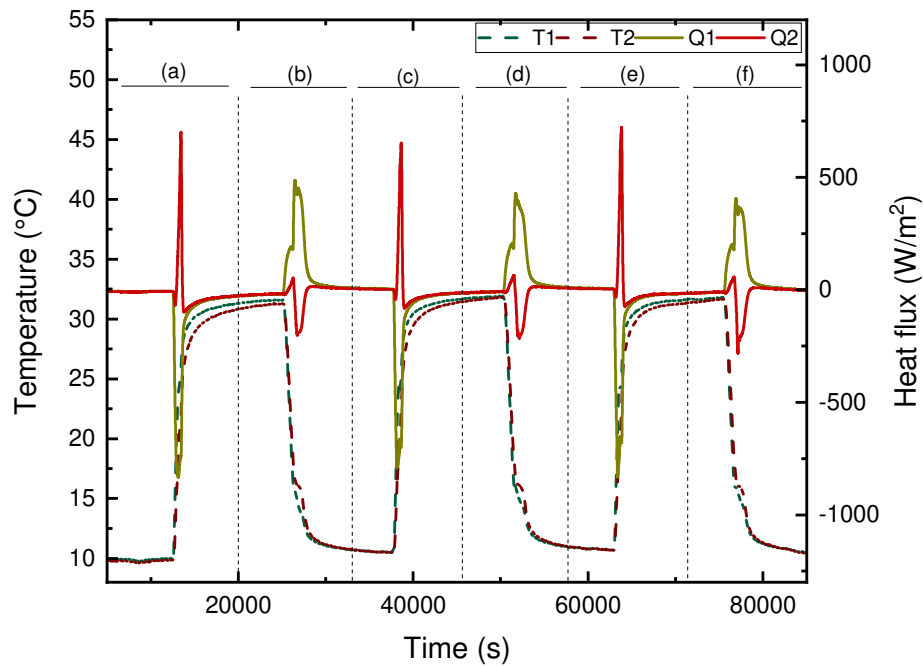

Fig. 9. Successive ramps of selected temperatures for a day.

Table 4 summarizes the measured stored and released heat energies of the composites with different hexadecane contents. This amount can also be obtained three times during the storage process and three times during the release process. In each cycle, there was almost no significant

change in the quantity of heat stored/released by the composites. It approves the stability of the composite. It was observed that thermal energy without graphite decreased with increasing hexadecane loading. On the other hand, the increase of the EG positively influenced the energy stored and released.

Table 4: Amount of energy stored or released in each cycle.

	Cycles	Stored energy (kJ/kg)	Released energy (kJ/kg)
S0	1	210.47	209.44
	2	209.22	206.54
	3	208.54	207.28
S1	1	128.19	122.49
	2	127.68	122.43
	3	127.84	122.16
S2	1	100.90	98.95
	2	100.59	98.23
	3	100.49	98.42
S3	1	204.56	200.31
	2	208.58	203.20
	3	206.17	201.94
S4	1	199.80	195.74
	2	199.31	196.26
	3	199.51	198.51
S5	1	218.98	216.20
	2	218.31	216.55
	3	217.98	215.95
S6	1	100.61	98.17
	2	100.81	98.53
	3	100.09	98.30
S7	1	120.83	117.83
	2	121.26	117.87
	3	120.04	118.05
S8	1	130.87	126.02
	2	130.31	126.12
	3	129.09	126.47

3.6.1 Latent heat thermal energy storage (LHTES)

The latent heat is one of the most important parameters in the selection of PCM for TES applications. It can be estimated by the total heat (Q) stored/released determined for a temperature variation from 10°C to 33°C. Between these two positions, the composite stored and

released a sensible (Q_{sens}) and latent (L_m) heats. The latent heat is calculated by subtracting the sensible heat from the total amount of heat [36, 37].

$$Q_{tot} = Q_{sens} + L_m = \left(C_{P_s}.\Delta T_s + C_{P_l}.\Delta T_l\right) + L_m \qquad \text{[KJ/kg]} \qquad (6)$$

Where C_{ps} and C_{pl} are the heat capacities of the composite at solid and liquid state, respectively, ΔT_s and ΔT_l are the temperature variations in solid and in liquid states and L_m is the latent heat per unit mass of the composites. Comparing the theoretical latent heat data of the composites, the latent heat of thermal storage of composites without GE (L_m sample) can be calculated by multiplying the latent heat of pure hexadecane (L_m hex) with its mass fraction in the composite (h).

$$Lm_{sample} = h.Lm_{Hex} \qquad (7)$$

Fig.10 gives a comparison between the actual and the theoretical latent heats of composites thermal storage without EG. As for the composite latent heat, it was influenced by the LDPE/SEBS content, which can be allocated to the fact that the introduction of LDPE/SEBS causes a corresponding decrease of Hexadecane content. In addition, in the LDPE/Hexadecane/SEBS composite only hexadecane can store / release latent heat by undergoing phase transition. These results show that the actual enthalpies are ultimately consistent with theoretical values.
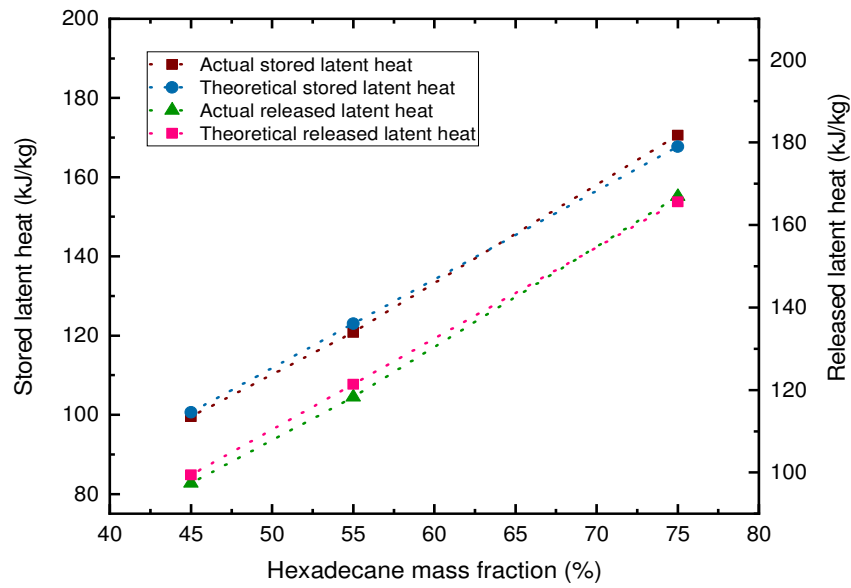
Fig. 10. Latent heat of composites: comparison of the theoretical and actual values.

Fig.11 and **Fig.12** compare the amount of heat stored by latent heat in composites with various expanded graphite loadings. It is clear that the composite latent heat with various mass fractions of EG is greater than composites without EG. The melting and solidifying latent heat of S0 composite are measured to be 170.56 and 168.32 J/g, which were inferior to these of S3, S4 and S5.
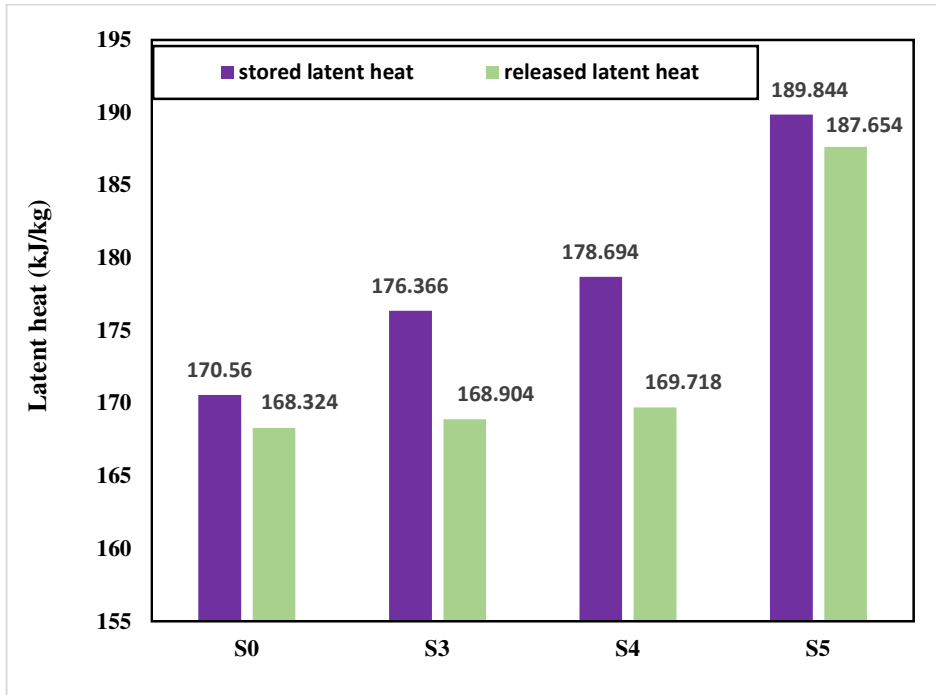
Fig. 11. Stored and released latent heats of composites: S0, S3, S4 and S5.
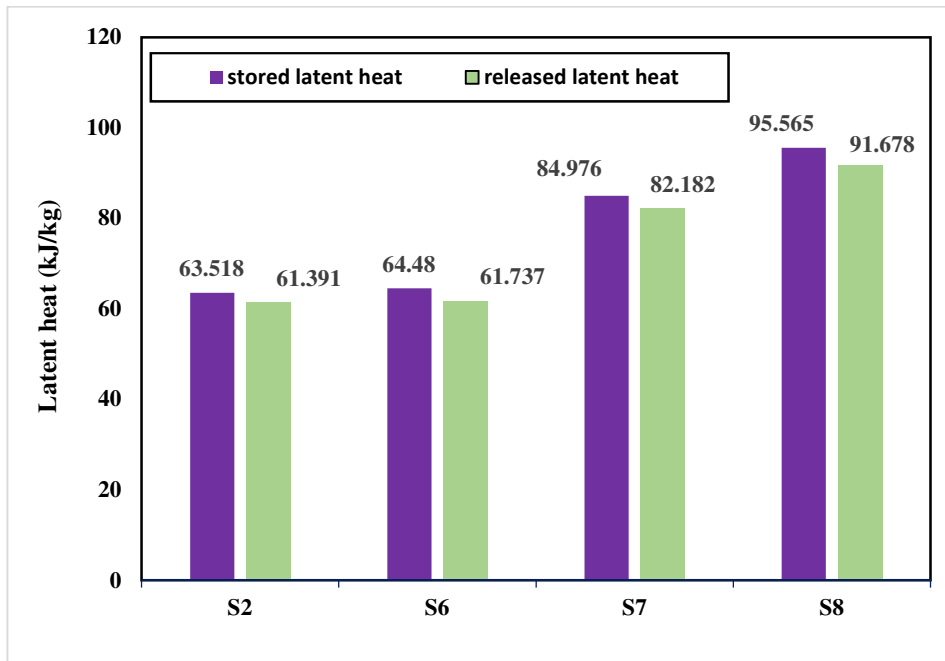

Fig. 12. Stored and released latent heats of composites: S2, S6, S7 and S8.

Fig.13 compares the time required for the hexadecane melting and solidification processes in the composites without and with EG. As can be seen, compared to the storage energy, the energy

release was a very long process and the solidification time was much longer than the melting process. Without expanded graphite (Fig. 13 b), this time is 1.42 h for melting and 2.42 h for solidification. This result is mainly attributed both to the rigidity and to the lower effective thermal conductivity of the SEBS/LDPE matrix. The rigidity induces high thermal contact resistance between the composite and the heat exchange plate. In the second hand, the solidification/melting cycles generate a thin layer of Hexadecane on the upper surface and in the depth of the composite. This slight layer ''insulates'' the liquid hexadecane from the cooling source [38] and reduce the effect of the convection mode. Obviously, this phenomenon can be also explained by the crystalline destruction of hexadecane during the transition from solid to liquid states [39].
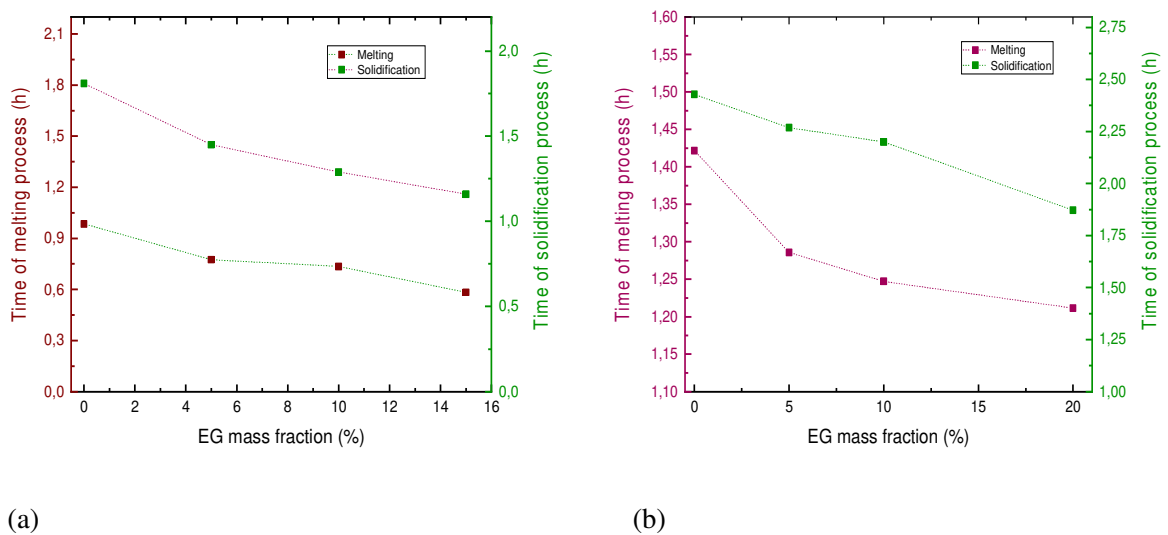

(a)   (b)

Fig. 13. Time needed to reach the temperature equilibrium state of different composites; (a) with 75 wt. % Hexadecane and (b) with 45 wt. % hexadecane.

We can observe from this figure that the high thermal conductivity of EG allows the thermal energy to flow quickly through the blend, reaching the PCM. The advantage of this configuration is to combine a high storage capacity and high heat propagation rate. The solidification time of the composite with 75 wt. % hexadecane decreased from 1.81 h to 1.16 h with greater loading of EG (0- 15wt. %). According to the above results, it can be concluded that the heat during cooling does not "overlap" to heat transfer during heating. This phase shift is useful for applications such

as building insulation or the cooling of electronic backdating. This phenomenon can be affected by many factors, namely, asymmetric effective thermal conductivity thermal conduction, natural convection and thermal contact resistance.

Conclusion

In this paper, a new composite, LDPE/Hexadecane/SEBS loaded with the EG were prepared for high thermal conductivity and to surmount the leakage of hexadecane, using the sonication method. LDPE served as a strong supporting material, while elastomer (SEBS) exhibited good encapsulation to Hexadecane and the EG was the additives for thermal conductivity enhancement. The composite is endowed with several important thermal properties. There was also no chemical reaction between SEBS, LDPE, Hexadecane and EG. A good compatibility was found between the composite's components. Moreover, the leakage test result proved that the prepared composite with 10% EG and 75wt. % hexadecane has an exceptional ability to hinder PCM leakage. Thus, we conclude that the EG improves the shape stability of composites with an important amount of hexadecane. The TGA results proved that all composites presented a good stability at the working temperature range. Apart from a positive effect on the shape stability, EG contributed to improving the heat transfer of the composite in both phases. The thermal conductivity intensification of the composite with 75 wt. % hexadecane increased from 38 to 277 % with greater loading of EG (5- 15wt. %). Similar data were noticed for composites with 45 wt. % hexadecane which had a maximum intensification of 351 % with 20 wt. % EG. Consequently, the latent heat capacity of LDPE/Hexadecane/SEBS/EG increase with the raising of EG content. The little amount of the thermal conductor diminished the melting and solidification times.

Overall, the prepared composites have the advantages of important heat storage ability, thermal conductivity, thermal stability and form stability. The results approve that the as-prepared composites have a good potential for advanced application like the thermal energy storage and management systems. Accordingly, studying the mechanical properties represents an interesting background for future work.

References

[1] B. Zalba, J.M. Marin, L. F. Cabeza, H. Mehling. Review on thermal energy storage with phase change: materials, heat transfer analysis and applications. APPL THERM ENG 2003; 23: 251-283.

[2] P.H. Feng, B.C. Zhao, R.Z. Wang. Thermo-physical heat storage for cooling, heating, and power generation: A review. APPL THERM ENG 2020; 166: 114728.

[3] L. Yaxue, J. Yuting, A. Guruprasad, F. Guiyin. Review on thermal conductivity enhancement, thermal properties and applications of phase change materials in thermal energy storage. RENEW SUSTENERG REV 2018; 82: 2730-2742.

[4] S. E. Kalnæs, B. P. Jelle. Phase change materials and products for building applications: A state-of-the-art review and future research opportunities. ENERG BUILDINGS 2015; 94: 150-176.

[5] M. M. Umair, Y. Zhang, K. Iqbal, S. Zhang, B. Tang. Novel strategies and supporting materials applied to shape-stabilize organic phase change materials for thermal energy storage–A review. APPL ENERG 2019; 235: 846-873.

[6] N. Soares, J. J. Costa, A. R. Gaspar, P. Santos. Review of passive PCM latent heat thermal energy storage systems towards buildings' energy efficiency. ENERG BUILDINGS 2013; 59: 82-103.

[7] P. Zhang, X. Xiao, Z.W. Ma. A review of the composite phase change materials: Fabrication, characterization, mathematical modeling and application to performance enhancement. APPL ENERG 2016; 165: 472–510.

[8] X. Huang, X. Chen, A. Li, D. Atinafu, H. Gao, W. Dong, G. Wang, Shape-stabilized phase change materials based on porous supports for thermal energy storage applications. CHEM ENG J 2019; 356: 641-661.

[9] B. He, V. Martin, F. Setterwall. Liquid–solid phase equilibrium study of tetradecane and hexadecane binary mixtures as phase change materials (PCMs) for comfort cooling storage. FLUID PHASE EQUILIBR 2003; 212: 97-109.

[10] J. N. Shi, M.D. Ger, Y. M. Liu, Y.C. Fan, N.T. Wen, C. K. Lin, N. W. Pu. Improving the thermal conductivity and shape-stabilization of phase change materials using nanographite additives. CARBON 2013; 51: 365-372.

[11] Z. Zhang, G. Alva, M. Gu, G. Fang. Experimental investigation on n-octadecane/polystyrene/expanded graphite composites as form–stable thermal energy storage materials. ENERGY 2018; 157: 625-632.

[12] X. Huang, C. Zhu, Y. Lin, G. Fang. Thermal properties and applications of microencapsulated PCM for thermal energy storage: A review. APPL THERM ENG 2019; 147: 841-855.

[13] Y. Zhang, J. Xiu, B. Tan, R. Lu, S. Zhang. Novel semi-interpenetrating network structural phase change composites with high phase change enthalpy. AIChE J 2018; 64: 688–696.

[14] L. Wang, D. Meng. Fatty acid eutectic/polymethyl methacrylate composite as form-stable phase change material for thermal energy storage. APPL ENERG 2010; 87: 2660-2665.

[15] L. Zhang, J. Zhu, W. Zhou, J. Wang, Y. Wang. Characterization of polymethyl methacrylate/polyethylene glycol/aluminum nitride composite as form-stable phase change material prepared by in situ polymerization method. THERMOCHIM ACTA 2011; 524: 128-134.

[16] Y. Wang, B. Tang, S. Zhang. Novel organic solar thermal energy storage materials: efficient visible light-driven reversible solid–liquid phase transition. J MATER CHEM 2012; 22: 18145-18150.

[17] I. Krupa, G. Miková, A. S. Luyt. Polypropylene as a potential matrix for the creation of shape stabilized phase change materials. EUR POLYM J 2007; 43: 895-907.

[18] M. Mu, P.A.M. Basheer, W. Sha, Y. Bai, T. McNally. Shape stabilized phase change materials based on a high melt viscosity HDPE and paraffin waxes. APPL ENERG 2016; 162: 68-82.

[19] I. Krupa, Z. Nógellová, Z. Špitalský, M. Malíková, P.Sobolčiak, H. W. Abdelrazeq, M. Ouederni, M. Karkri, I. Janigová, M. A.S A. Al-Maadeed, Positive influence of expanded

graphite on the physical behavior of phase change materials based on linear low-density polyethylene and paraffin wax. THERMOCHIM ACTA 2015; 614: 2018-225.

[20] P. Sobolciak, M. Mrlík, M.A. AlMaadeed, I. Krupa. Calorimetric and dynamic mechanical behavior of phase change materials based on paraffin wax supported by expanded graphite. THERMOCHIM ACTA 2015; 617: 111-119.

[21] K. Merlin, D. Delaunay, J. Soto, L. Traonvouez. Heat transfer enhancement in latent heat thermal storage systems: Comparative study of different solutions and thermal contact investigation between the exchanger and the PCM. APPL ENERG 2016; 166: 107-116.

[22] I. Chriaa, A. Trigui, M. Karkri, I. Jedidi, M. Abdelmouleh, C. Boudaya. Thermal properties of shape-stabilized phase change materials based on Low Density Polyethylene, Hexadecane and SEBS for thermal energy storage. APPL THERM ENG 2020; 171: 115072.

[23] W. Wu, W. Wu, S. Wang. Form-stable and thermally induced flexible composite phase change material for thermal energy storage and thermal management applications. APPL ENERG 2019; 236: 10-21.

[24] L. Colla, L. Fedele, S.Mancin, L. Danza, O. Manca. Nano PCMs enhanced energy storage and passive cooling applications. APPL THERM ENG 2017; 110: 584-589.

[25] A. Trigui, M. Karkri, C. Boudaya, Y. Candau, L. Ibos, M. Fois. Experimental investigation of a composite phase change material: thermal-energy storage and release. J COMPOSMATER 2014; 48: 49–62.

[26] A. Trigui, M. Karkri, C. Boudaya, Y. Candau, L. Ibos. Development and characterization of composite phase change material: thermal conductivity and latent heat thermal energy storage. COMPOSPART B-ENG 2013; 49: 22–35.

[27] M.Karkri, M. Lachheb, F. Albouchi, S. B. Nasrallah, I. Krupa. Thermal properties of smart microencapsulated paraffin/plaster composites for the thermal regulation of buildings. ENERG BUILDINGS 2015; 88: 183-192.

[28] C. Moulahi, A. Trigui, M. Karkri, C. Boudaya. Thermal performance of latent heat storage: Phase change material melting in horizontal tube applied to lightweight building envelopes. COMPOS STRUCT 2016; 149: 69-78.

[29] M. Karkri, M. Lachheb, Z. Nógellová, B. Boh, B. Sumiga, M. A. AlMaadeed, A. Fethi, I. Krupa. Thermal properties of phase change materials based on high-density polyethylene filled with micro-encapsulated paraffin wax for thermal energy storage. ENERG BUILDINGS 2015; 88: 144-152.

[30] M. A. AlMaadeed, S. Labidi, I. Krupa, M. Karkri. Effect of expanded graphite on the phase change materials of high-density polyethylene/wax blends. THERMOCHIM ACTA 2015; 600:35-44.

[31] S. Kim, S. Jin Chang, O. Chung, S.G. Jeong, S. Kim. Thermal characteristics of mortar containing hexadecane/xGnP SSPCM and energy storage behaviors of envelopes integrated with enhanced heat storage composites for energy efficient buildings. Energy and Buildings 2014; 70: 472-479.

[32] Y. Lin, C. Zhu, G. Alva, G. Fang. Palmitic acid/polyvinyl butyral/expanded graphite composites as form-stable phase change materials for solar thermal energy storage. APPL ENERG 228; 2018: 1801-1809.

[33] P. Sobolciak, M. Karkri, M. A. Al-Maadeed, I. Krupa. Thermal characterization of phase change materials based on linear low-density polyethylene, paraffin wax and expanded graphite. RENEW ENERG 2016; 88: 372-382.

[34] M. A. AlMaadeed, S. Labidi, I. Krupa, M. Karkri. Effect of expanded graphite on the phase change materials of high-density polyethylene/wax blends. THERMOCHIM ACTA 2015; 600: 35-44.

[35] A. Joulin, L. Zalewski, S. Lassue, H. Naji. Experimental investigation of thermal characteristics of amortar with or without a micro-encapsulated phase change material. APPL THERMENG 2014; 66: 171-180.

[36] W. Wu, G. Zhang, X. Ke, X. Yang, Z. Wang, C. Liu, Preparation and thermal conductivity enhancement of composite phase change materials for electronic thermal management. ENERG CONVERS MANAGE 2015; 101: 278-284.

[37] L. Xia, P. Zhang, R.Z. Wang, Preparation and thermal characterization of expanded graphite/paraffin composite phase change material, CARBON 2010; 48; 2538–2548.

[38] D. Juárez, S. Ferrand,O. Fenollar, V. Fombuena, R. Balart. Improvement of thermal inertia of styrene–ethylene/butylene–styrene (SEBS) polymers by addition of microencapsulated phase change materials (PCMs). EUR POLYM J 2011 ; 47 : 153-161.

[39] P. Chen, X. Gao, Y. Wang, T. Xu, Y. Fang, Z. Zhang. Metal foam embedded in SEBS/paraffin/HDPE form stable PCMs for thermal energy storage. SOL ENERG MATSOL C 2016; 149: 6-65.
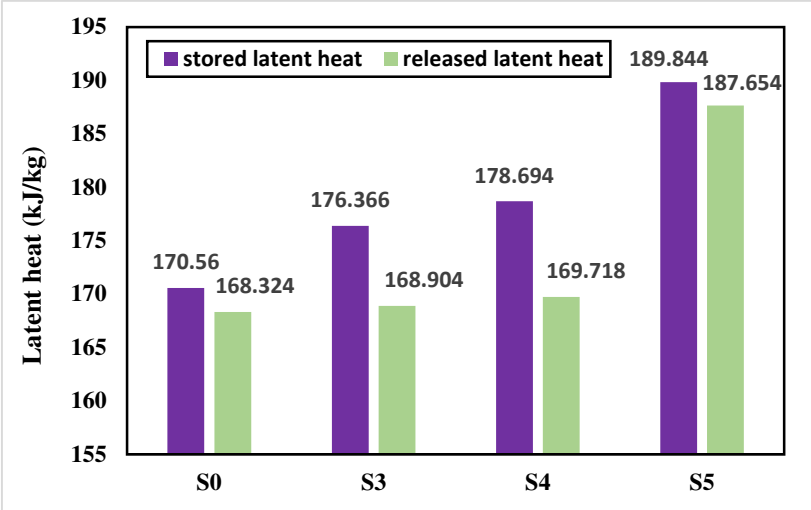
Fig. 1. Stored and released latent heat of composites